

# The difference in the slope supported system when excavating twin tunnels: Model test and numerical simulation

Xinrong Liu<sup>1,2,3</sup>, Lojain Suliman<sup>1,2,3</sup>, Xiaohan Zhou<sup>\*1,2,3</sup>, Jilu Zhang<sup>1,2,3</sup>, Bin Xu<sup>1,2,3</sup>,  
Fei Xiong<sup>1,2,3</sup> and Ahmed Abd Elmageed<sup>4</sup>

<sup>1</sup>College of Civil Engineering, Chongqing University, Chongqing 400045, China

<sup>2</sup>State Key Laboratory of Coal Mine Disaster Dynamics and Control, Chongqing University, Chongqing 400044, China

<sup>3</sup>National Joint Engineering Research Center of Geohazards Prevention in the Reservoir Areas (Chongqing), Chongqing 400045, China

<sup>4</sup>National Authorities for Tunnels, Egypt

(Received July 26, 2022, Revised August 31, 2022, Accepted September 12, 2022)

**Abstract.** Slope stability during the excavation of twin road tunnels is considered crucial in terms of safety. In this research, physical model testing and numerical analysis were used to investigate the characteristics of the settlement ( $uz$ ) and vertical stresses ( $\sigma_z$ ) along the two tunnel sections. First, two model tests for a (fill-rock) slope were conducted to study the settlement and stresses in presence and absence of slope support (plate support system). The law and value of the result were then validated by using a numerical model (FEM) based on the physical model. In addition, a finite element model with a slope supported by piles (equivalent to the plate) was used for comparison purposes. In the physical model, several rows of plates have been added to demonstrate the capacity of these plates to sustain the slope by comparing excavating twin tunnels in supported and unsupported slope, the results show that this support was effective in the upper part of the slope, while in the middle and lower part the support was limited. Additionally, the plates appear to induce less settlement in several areas of the slope with differing settlement and stress distribution as compared to piles. Furthermore, as a results of the previous mentioned investigation, there are many factors influence the stress and settlement distribution, such as the slope's cover depth, movement during excavation, buried structures such as the tunnel lining, plates or piles, and the interaction between all of these components.

**Keywords:** model test; numerical simulation; plates; slope stability; twin tunnels

## 1. Introduction

Increasing of the population, the extension of urbanization and the development of living standards lead to traffic problems. Hence the need for the evolution of the urban transport network increases. Subsequent to this, tunneling in dense cities that include soil materials has become substantially. In recent decades, two tunnels excavation and construction have become very common in many high dense population cities (Chen *et al.* 2011, Elwood and Martin 2016, Gao *et al.* 2017, Wang *et al.* 2019, Shiver *et al.* 2020, Suwansawat and Einstein 2007, Nematollahi and Dias 2020, Nematollahi and Dias 2019).

Settlement is an unavoidable problem in the excavation, construction of the tunnels and underground spaces which are close to the ground's surface. To investigate the ground displacement caused by single tunnel, Field observation has been used (Peck 1969, Cording 1975). Analytical method (Loganathan and Poulos 1998, Bobet 2001), numerical modelling (Rowe *et al.* 1983, Addenbrooke 1996, Franzius *et al.* 2005). Physical modelling (Taylor 1984, Huang *et al.* 2013).

Moreover, the twin tunnels in flat land have been

studied by many researchers by using numerical modelling investigations (Chen *et al.* 2009, Mortazavi *et al.* 2009, Chakeri *et al.* 2011, Ocak 2013, Oliaei and Manafi 2015, Channabasavaraj and Visvanath 2013, Li *et al.* 2013, Li and Ji 2017, Wu *et al.* 2020). Relatively speaking, also many studies have investigated twin tunnels issue through a physical model (Choi and Lee 2010, Kim 2012, Seo *et al.* 2014, Yang *et al.* 2017, Zheng *et al.* 2021). However, very few studies have looked at the settlement due to excavate twin tunnels in a slope by using physical models. Ma (2015) used finite difference software (FLAC3D) to model the building of a loess tunnel and explore the variables that influence settlement in mountain areas. (Vlachopoulos and Vazaios, 2015) used a 2D numerical model to study two tunnels excavating interaction within slope in weak rock mass by a case study and found that the 2D design is crude enough in the preliminary stage of construction. He *et al.* (2020) studied the influence law of existing tunnels on the construction of intersecting new tunnels in a shallow slope through 3D numerical analysis, the simulations revealed that a critical interval length must exist between the two tunnel lines. Zhang *et al.* (2019) investigated the interaction law of twin tunnels excavation and slope stability by using model test and numerical simulation, they found that the influence area of tunnel excavation on the deformation of the slope range from 1.5 times of the tunnel span, which should be well strengthened and monitored. Excavation events on slope stability are therefore one of the most

\*Corresponding author, Associate Professor  
E-mail: zhouxh2008@126.com

important problems relating to surface settlement, and these events have a significant impact on operational reliability both during and after execution.

Furthermore, many previous studies have been mentioned the pile tunnel interaction issues. Such as: Soomro *et al.* (2020) studied the influence of construction sequence of twin stacked tunneling on existing pile. Ng *et al.* (2013) investigated the interaction between tunnel and existing pile. Nematollahi and Dias (2019) made three dimensional numerical simulations to investigate the tunnel pile interaction. Soomro *et al.* (2017) studied the response of a pile to side by side twin tunnels in saturated stiff clay. Soomro (2021) made a 3D numerical modelling using an advanced hypo plasticity soil model to investigate the response of an existing (2×2) piles raft to twin stacked tunneling at various depth. Hong *et al.* (2015) made a centrifuge model test to simulate the side by side twin tunnels with pile group at two critical locations relative to the pile group. However, none of the previous studies mentioned the interaction between a plate and twin tunnel in a slope during excavation or making comparison between the difference between using a pile and plate as a support system.

A physical model for twin tunnels in a slope has been investigated in two cases in this article. The first is to use (plates) to stabilize the slope while digging the twin tunnels. The second task is to dig the twin tunnels without any assistance (without plates). Furthermore, to establish a comparison between the results, 3D finite element analysis (FEM) was used to validate the findings of the physical model. In addition, to make a numerical model to simulate the presence of the piles in equivalent characteristic to the plate, to illustrate the difference in the function of each support system. Moreover, an analytical solution includes new equation has been used for the none-supported slope in order to make verification with the numerical simulation.

## 2. Physical model tests

### 2.1 The original idea of the model test

#### 2.1.1 Project description

This case study locates in Guizhou province in Kaili city in southwest china.this city has a big population, which leads to construct many tunnels. The soil profile consists of two layers, the first one is limestone rock, while the second one is fill soil. at The back part of the fill the roadbed of Lubixi Road is located, and the roadbed consists of limestone block gravel and clay, with a medium to dense structure.

#### 2.2.2 Geological conditions

The landform of Luobang Tunnel site is a dissolution-erosion type low-middle mountain landform. The surface is strongly corroded and eroded, and the terrain is undulating. There is no surface water such as surface runoff and weir ponds in the tunnel site. The surrounding rock of the entrance section of the tunnel is moderate-breeze limestone with soft rock texture,  $R_c=20$  MPa. The joints of rock mass are relatively developed-undeveloped, the rock mass is

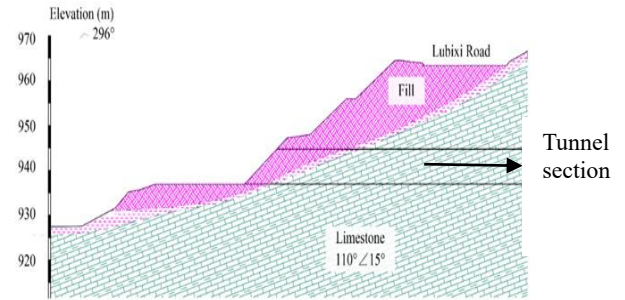


Fig. 1 Geological profile for case under study

Table 1 similarity coefficient ratio

Parameters	Proto type	Model test	definition	Similarity coefficient
Density	$\rho_p$	$\rho_m$	$c_p = \frac{\rho_p}{\rho_m}$	1
Cohesion	$c_p$	$c_m$	$c_c = \frac{c_p}{c_m}$	100
Friction angel	$\Phi_p$	$\Phi_m$	$c_\Phi = \frac{\Phi_p}{\Phi_m}$	1
Stresses	$\sigma_p$	$\sigma_m$	$c_\sigma = \frac{\sigma_p}{\sigma_m}$	100
Modulus of elasticity	$E_p$	$E_m$	$c_E = \frac{E_p}{E_m}$	100
Poisson ratio	$\mu_p$	$\mu_m$	$c_\mu = \frac{\mu_p}{\mu_m}$	1

relatively complete. The loose fill is located on the entrance slope of Luobang Tunnel. The fill is formed by the construction waste of Lubixi Road. The main components are limestone blocks and clay.

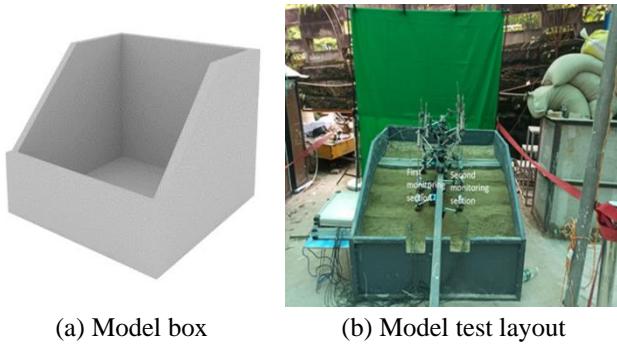
### 2.2 The law of similarity and material of ground

Physical models must satisfy a series of similarity requirements in terms of geometry, physical-mechanical properties, boundary conditions, and initial stress conditions (Fumagalli 2013, Zhu *et al.* 2010). However, it is difficult to satisfy all the similar constant (Lü *et al.* 2018, Sun *et al.* 2018). Thus it is very important to choose the suitable similar ratio. The reduced scale of dimension  $C_l$  in the model tests was selected as (100). The general law of similarity between the prototype parameters and the model parameters may be derived according to the similarity theory, as illustrated in Table 1.

$$C_l = \frac{i_p}{i_m} \quad (1)$$

Herein, the subscript “p” represents the prototype and “m” represents the test model. Since a mixture of artificial materials has been proved to be appropriate for a scaled model test Meguid *et al.* (2008). In this research, a model material is created to meet the scaled test criteria, which is a combination of quartz sand, barite, and water. According to the similarity theory (Jiang 1993), the model and prototype must satisfy the different equations of equilibrium, thus the following similarity index requirement should be met.

$$C_\sigma = C_L C_l$$



(a) Model box (b) Model test layout

Fig. 2 Model box and sensors layout



(a) Mixing the material (b) preparing sensors

Fig. 3 Preparing the model test

$$\begin{aligned} C_\sigma &= C_e C_\gamma \\ C_{e=c_\phi=c_u} &= 1 \end{aligned} \quad (2)$$

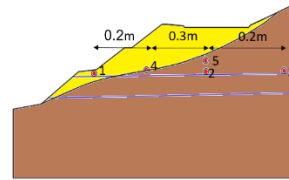
### 2.3 Apparatus of model tests and measurement

The model test was conducted in a steel box with dimensions  $1.2 \times 1.2 \times 0.8$  as seen in Fig. 2(a). while, Fig. 2(b) shows the model box filled with soil and rock material. The structural steel-wall is composed of steel plate which is connected by a high strength bolts. The distance from the boundary of the box to the tunnel side is more than 2.5 times of the tunnel span, so the boundary effect can be ignored Huang *et al.* (2013). Two steel tunnels were embedded in the soil to represent the tunnel support. The thickness of the lining has been calculated depending on the similarity law. Each lining has a thickness of 1mm. In order to simulate the loads on the road and according to the similarity ratio, the loads on the road were represented by distributed concrete bars with weights of  $0.25 \text{kn/m}^2$ . these loads have been distributed on the road as a surface loads. These loads have been represented by weights. They were determined and weighed before they have been used. Then, these loads have been distributed on the road.

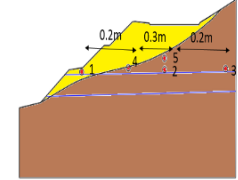
Two different digging techniques were used throughout the excavation: the first one was a small tool that was used to excavate the first section of the twin tunnel, and the other was a long tool that was used to excavate the remaining tunnels. Both tools are made of steel. In the model test, two kinds of soil (fill and rock) were utilized, and these two materials were manually poured and compacted layer by layer in the tank using a hammer to reach the required volume. Two steel tunnels were embedded in the soil. The loads on the road have been represented by distributed weights equal to  $0.25 \text{kn/m}^2$ , according to the similarity ratio. The clear distance between the twin tunnels was 0.21



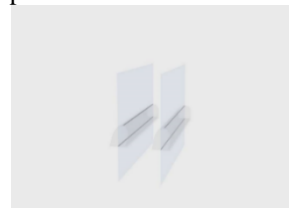
(a) Displacement sensor (b) Stress sensor



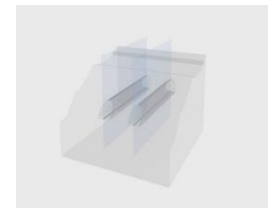
(c) Displacement sensor position



(d) Stresses sensor position



(e) Monitoring sections



(f) Long monitoring two sections of the tunnel

Fig. 4 Sensors types, positions and sections

m. the diameter of each tunnel is 0.13 m. The first 0.2 m of the first tunnel was dug initially, followed by the excavation of both tunnels at the same time. Preparing and mixing the material is shown in Fig. 3(a). As indicated in Fig. 4(a), 4(b), two types of sensors were used: displacement sensors and earth pressure sensors. These sensors have embedded in two main monitoring section along the length of each tunnel as shown in the parts of Fig. 4. The first one is located over the left tunnel, while the second is located above the right tunnel. As indicated in Fig. 4, the monitoring components are buried in the representative regions, and the arrangement of measurement points in the two monitoring sections is the same. It should be noted that prior to the model test, all monitoring components were thoroughly examined. The reason for laying out the sensors in this way related to the expectation that the maximum settlement will be in these two sections. Stress sensors and displacement sensors are shown in the two Figs. 4(c), 4(d) respectively.

### 2.4 Scheme of model tests

Two model experiments were carried out in this research to examine the tunnel's settlement ( $u_z$ ) and vertical stresses ( $\sigma_z$ ), as well as those in the surrounding soil and rock.

(1) test1: the vertical displacement (settlement) and stresses in unsupported slope

(2) test2: the vertical displacement (settlement) and stresses in supported-slope

It's worth noting that a steel plate of comparable thickness was utilized to depict the massive number of

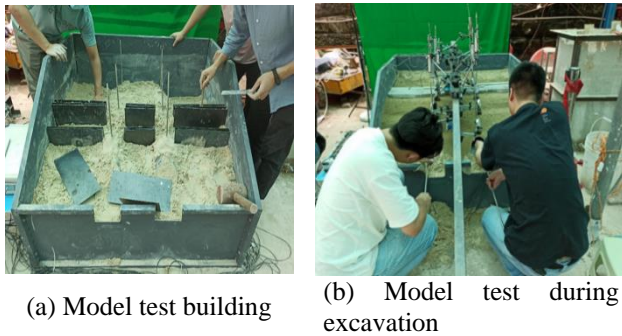


Fig. 5 Building and excavating model test procedure

Table 2 The material properties used in the model test

Material	$C$ (kpa)	$\Phi$ (deg)	$E$ (kN/m <sup>3</sup> )	$\mu$	$\lambda$ (KN/m <sup>3</sup> )
Fill	0.26	33	300	0.4	18
Rock	2	33	21000	0.2	24

piles. Three rows of plates in two inclined positions of the slope have been used, in addition to one row in the begging of the slope. Fig. 5(a) shows the right place of the plates. These plates have been placed after measuring the distance according to the determined distances. It has been noted that soil between the plates has been compacted due to the small distance between the plates. Furthermore, the soil which located between the steel lining and the plates also have been compacted. Fig. 5(b) shows the excavation procedure in the model test. It should be noted that all model test results, including displacement and stress, are converted into prototype values using a reduced scale. Table 2 shows the materials as have been used in the model test. The distance between the tunnel's start and the last excavation stage was measured using a remote control. The remote control will start the measuring from the beginning of the tunnel. Then, the distance from the begging of the tunnel till reaching the last excavation step will appear on the screen of the remote control. Each tunnel will be dug in a series of phases, each measuring 0.005 m in length. With customizing a relaxation time after each excavating phase. The relaxation time depends on the settlement action which appears on the screen. This screen shows the settlement movement. Thus the time between each two excavation steps will depend on the settlement behavior after each digging step.

### 3. Involved methodologies

#### 3.1 Numerical analysis

##### 3.1.1 FEM model

In this section, 3D numerical simulations analyses were performed to evaluate the settlement and vertical stresses characteristics. The geometry (height×width×length) of the numerical model was (120 m×120 m×65 m), corresponding to that the physical model was magnified 100 times (the reduced scale) to prototype size. The numerical calculations were carried out using the plaxis 3D finite element program.

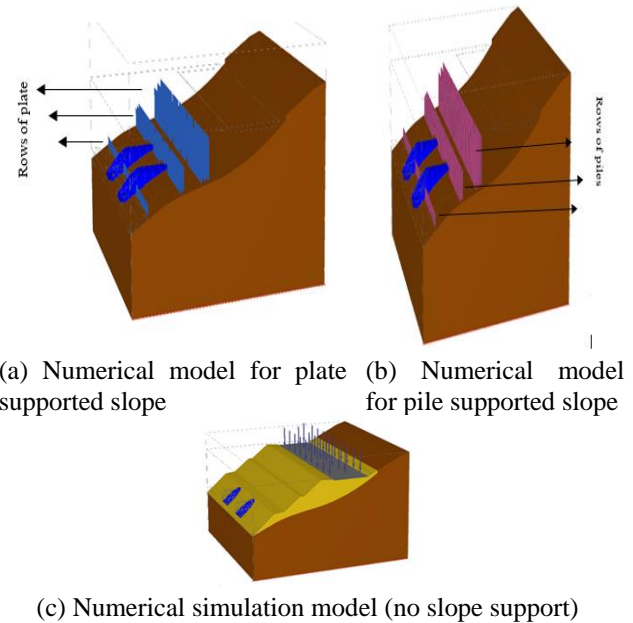


Fig. 6 Numerical simulation models used in the model test

Numerical models are shown in Fig. 6. The merit of computer simulation is, it is quick, powerful and less expensive Speers (1992). Finite element method (FEM) considers the excavation process in a step by step manner (Zhang *et al.* 2016). Thus a series of finite element models have been conducted, depending on many stages that may affect on the settlement and could be summarized in the following items. The model was fixed in the horizontal direction at each side and the bottom part of the boundary was fixed in all directions. The top surface of the model was free in all directions. After sensitivity analysis the mesh has been considered as a medium size.

#### 3.1.2 General

A series of 3D finite element models (FEM) have been conducted and compared with experiment model test (physical model) to evaluate the vertical settlement (UZ) and vertical stresses due to excavate twin tunnels in many conditions. These conditions have been studied in details and include:

- excavating twin tunnels without any support.
- excavating twin tunnels with piles as a support for the slope.
- using plate instead of piles to excavate the two hole of tunnels.

These three major models have been analyzed and compared one by one in many sections. the purpose of this comparison was to investigate how the piles affect the tunnel excavation and to know the difference between using piles and plate to support the slope. As indicated in Fig. 6, the piles the same as the plates, were placed in three rows under the road section in the upper part of the inclined portion of the slope, three rows in the middle section of the slope, and one last section at the start of the slope. The distance between the piles in the horizontal direction is (1 m). while in the other direction was (2 m, 1 m) for the first and second three rows respectively. Fig. 6 shows the FEM

Table 3 The parameters used in the numerical simulation process

Material	C (KPA)	Φ (degree)	E (kN/m <sup>2</sup> )	μ	γ (kN/m <sup>3</sup> )
fill	26	33	30000	0.4	18
rock	200	33	2100000	0.2	24

Table 4 The pile properties in the numerical simulation (FEM)

E (KN/m <sup>2</sup> )	γ (KN/m <sup>3</sup> )	D (m)
30000000	25	0.6

Table 5 The plate properties used in the numerical simulation (FEM)

E (KN/m <sup>2</sup> )	γ (KN/m <sup>3</sup> )	Thickness (m)
200000000	78.5	0.2

models for the previous mentioned three cases.

### 3.1.3 Constitutive model and soil parameters

Mohr- columb model Mohr (1914) uses usually for soils and rock mechanic Zhao (2000). (Vlachopoulos and Vazaios) used mohr-columb for rocks in a slope with twin tunnels. Ağbay and Topal (2020) also used mohr columb in phase simulation software, to simulate the rock action. In this research paper mohr-columb model has been used for both the fill and rock, as an elastic perfectly plastic constitutive models. The parameters of the soil are obvious in the Table 3. While the Tables 4, 5 show the propertied of the plate and piles.

Common form of M-C yield criterion is

$$\tau = C + \sigma \tan \Phi \quad (3)$$

Mohr coulomb usually expressed in terms of stress invariants

$$(\sigma_1 - \sigma_3)/2 = \sin \Phi [(\sigma_1 + \sigma_3)/2 + C \cot \Phi] \quad (4)$$

The plate equivalent to the piles will be according to

$$EI(\text{plate}) = EI(\text{pile}) \quad (5)$$

Where: C: is the cohesion Φ: is the friction angel

E: is elasticity modulus μ: is poisson ratio

γ: is unit weight

The shotcrete modeled as a plate element with thickness of 0.28 m and unit weight of 25 kN/m<sup>2</sup> and the modulus of elasticity of 10.5 GPa.

### 3.1.4 Stage construction

The stages of construction include many steps. The first one was to analyze the initial phase depends on gravity loading because the land is not horizontal and including a slope. Then analyzing the road under the effect of distributed loads which represented as a surface loads according to Chinese code with a value of (25 kN/m<sup>2</sup>). These loads have been simulated after the initial phase without any type of excavation. As the excavation has been started at specific level, the interaction between the twin tunnels will influence the vertical displacement and another

aspect. The excavation of the two tunnels began in the third stage with the use of the “full face technique”. As in the model test the excavation in the numerical simulation has been started in the left one, till reach 20 meters then the next tunnel excavation has been started. This is what occurred in the physical model and what the finite element model simulated. The excavation in our case is a 3D problem due to the existing slope and the variation in the ground level. Each part has to be excavated in caution way, because if there is a part has been excavated instead of any other part, the results will not be accurate. Each segment of the tunnel has a width of 5meters.

## 3.2 Analytical solution

The superposition technique is recommended for estimating settling caused by twin tunnel excavation. In this approach, the settlement prediction is based on a single-tunnel prediction formula. The diameter, size and depth of the second tunnel is assumed to be the same as the first tunnel. This analytical formula contains two types of settlement: uniform convergence and ovalization. The flowchart which has been used in the programming process has been shown below. The properties of the fill and rock has been considered as an average of the two materials along the height of the slope.

Convergence mode

$$u_{xc} = u_{\epsilon} \frac{xR}{x^2 + y^2} \quad (6)$$

$$u_{yc} = u_{\epsilon} \frac{yR}{x^2 + y^2} \quad (7)$$

Ovalization mode

$$u_{yo} = u_{\delta} \frac{YR}{3 - 4\mu} \frac{(3 - 4\mu)((X^2 + Y^2)^2 - (3X^2 - Y^2)(X^2 + Y^2 - R^2))}{(X^2 + Y^2)^3} \quad (8)$$

$$u_{yo} = u_{\delta} \frac{YR}{3 - 4\mu} \frac{(3 - 4\mu)((X^2 + Y^2)^2 - (3X^2 - Y^2)(X^2 + Y^2 - R^2))}{(X^2 + Y^2)^3} \quad (9)$$

Where:

R the radius of the tunnel,

H the tunnel depth to the spring line,

μ The Poisson's ratio,

X the horizontal distance of the section,

X max.deformation due to

ovalization occurs at the tunnel cavity

u<sub>δ</sub> max.deformation due to

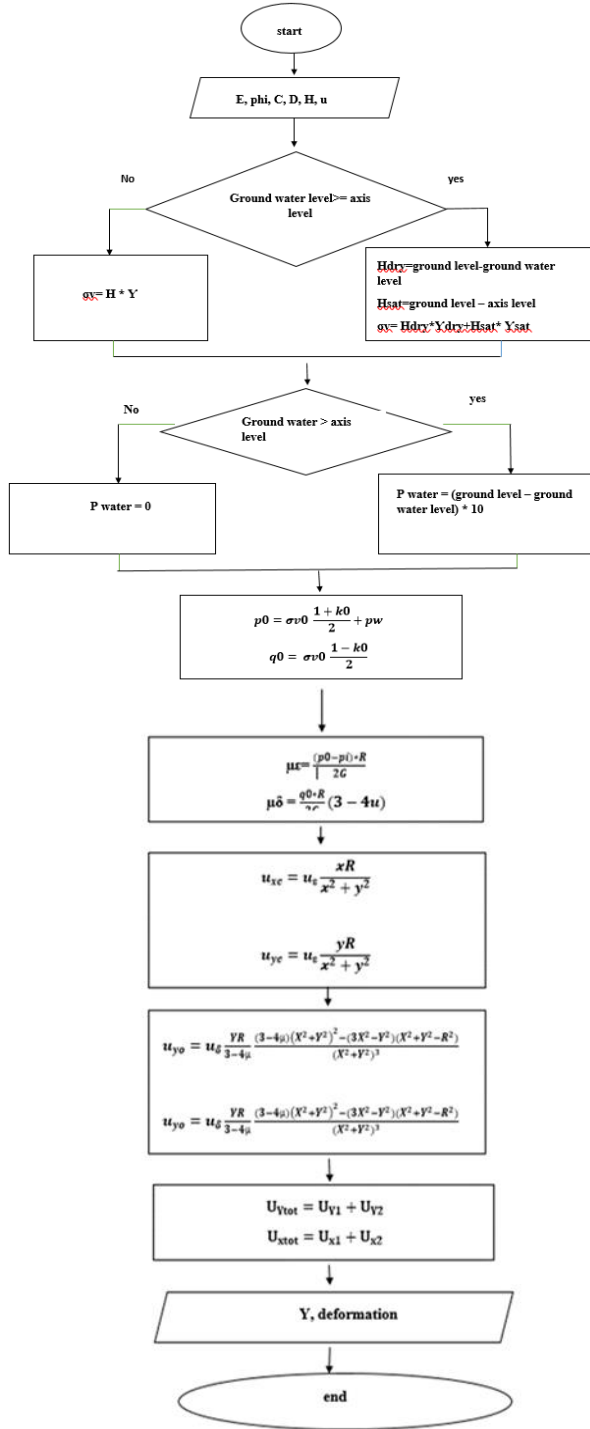
u<sub>ε</sub> convergence occurs at the tunnel cavity.

y the vertical distance of the section.

Based on the superposition principle, the settlement for two tunnels could be expressed as the following

$$U_{Ytot} = U_{Y1} + U_{Y2} \quad (10)$$

$$U_{xtot} = U_{x1} + U_{x2} \quad (11)$$



Where:

- $U_{y1}$  ( $U_{Y1} = U_{yc} + U_{y0}$ ): the first tunnel's vertical settlement (mm),
- $U_{y2}$  ( $U_{Y2} = U_{yc} + U_{y0}$ ): the second tunnel's vertical settlement (mm),
- $U_{yc}$  Settlement due to the convergence mode (mm),
- $U_{y0}$  Settlement due to the ovalization mode (mm),
- $U_{x1}$  ( $U_{X1} = U_{xc} + U_{x0}$ ): the first tunnel's horizontal settlement (mm),
- $U_{x2}$  ( $U_{X2} = U_{xc} + U_{x0}$ ): the second tunnel's horizontal settlement (mm),

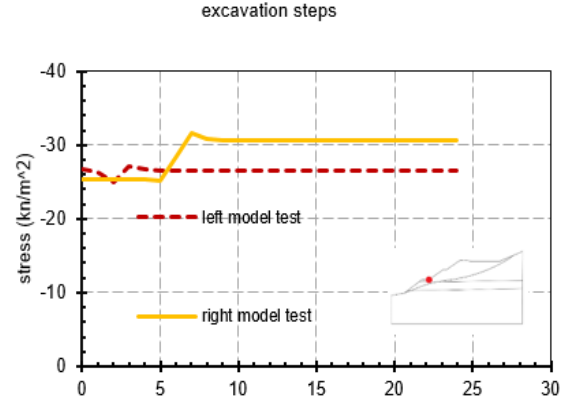


Fig. 7 Stresses in the first part of the tunnel tunnel-sensor position (1)

- $U_{xc}$  Settlement due to the convergence mode (mm),
- $U_{x0}$  Settlement due to the ovalization mode (mm).

## 4. Results

According to the results of the two monitoring sections along each tunnel. The stress variation and displacement behavior in many sensors position, depending on the sensors configuration as have been shown in Fig. 3 will be shown in the next charts. The results will be shown in two main parts. The first one when there is no support. And the another one when the rows of plates supported the slope. In addition to a discussion part which include many comparisons between the plate supported slope, pile supported slope and no support. Moreover, a comparison between the displacement ( $ux$ ) of the piles and plates have been done.

### 4.1 Slope with no support (numerical simulation-model test)

Many points have been monitored depending on the sensors position in both the displacement and stresses cases. The results show the following:

#### 4.1.1 vertical stresses

Five charts (7-11) show the stress variation in five points buried in the slope. The Figs. 7-9 represent the sensors which are directly above the tunnel and along each tunnel center. Fig. 7 shows the stress in the first part of the slope above the tunnel where the cover depth is too small (sensor 1). In this figure, it is obvious that after the excavation the stress has been increased in the two tunnels (right and left), this is may due to stress concentration in the lining after this area has been excavated due to the small cover depth in this region (slope high small). While Fig. 8 shows that after the excavation reach the sensor point the vertical stresses has been dropped down. This is normal due to stress release. The same happened in chart (9) which represent sensor (3). The next two figures represent the stresses in two sensors places little far from the tunnel lining. In Fig. 10 where the sensor point is in the inclined

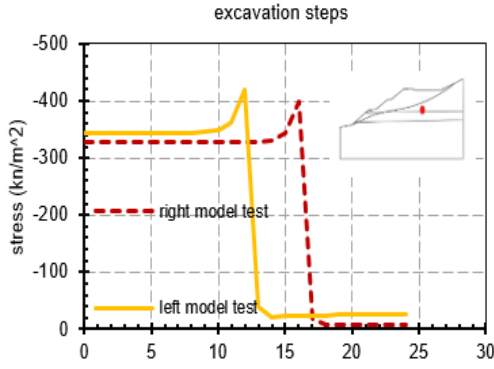


Fig. 8 Stresses in the middle part of the tunnel-sensor position (2)

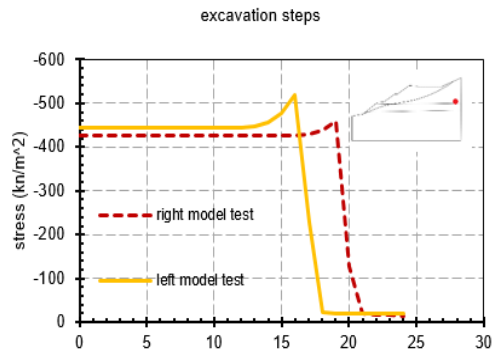


Fig. 9 Stresses in the last tunnel part of the tunnel-sensor position (3)

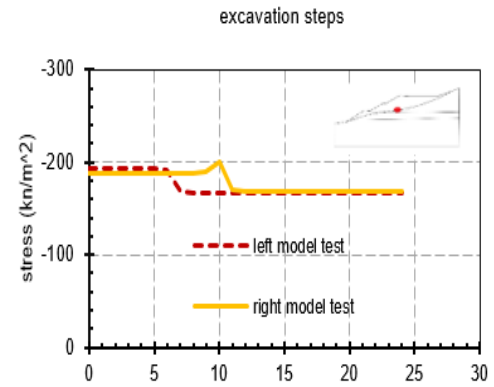


Fig. 10 Stresses in the inclined part of the slope-sensor position (4)

part of the slope and does not located directly above the tunnel the stress variation before and after excavation is less in comparison with the previous mentioned cases. While in chart (11) where there is a surface distributed load it is clear the settlement also has been dropped down. which leads to consider that the vertical stresses seem to diminish with the excavating action in the left and right tunnels, as illustrated in Figs. 8-9, while vertical stresses appear to rise in the non-excavated area. In addition, before the excavation reach the specific point the stress will be concentrated in this area because of high stiffness in the point comparing to release stresses in the excavated places.

The vertical ground pressure is induced by the self-weight of ground layers above the crown of the tunnel. The

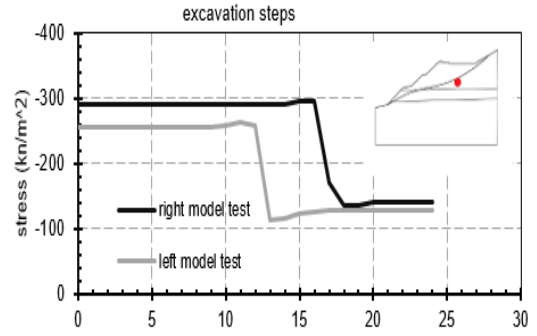


Fig. 11 Stresses under the road-sensor position (5)

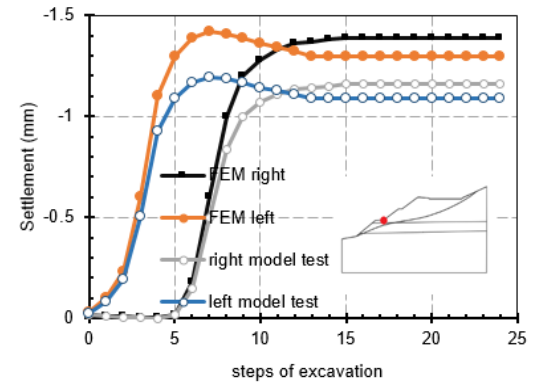


Fig. 12 Settlement in first of the tunnel-sensor point (1)

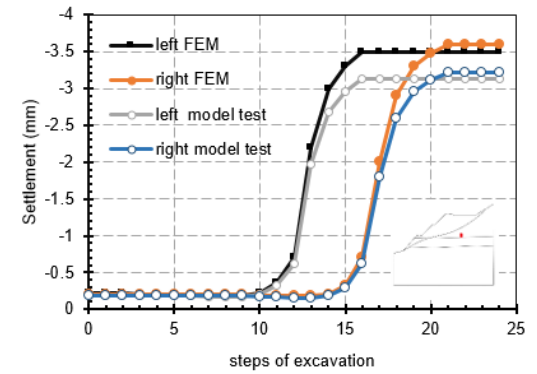


Fig. 13 Settlement in the middle part of the tunnel-sensor point (2)

vertical pressure equals the overburden pressure of the above layers as appear in this formula Yun (2019)

$$\sigma v = p_0 + \Sigma Y_i H_i + \Sigma Y_j H_j \quad (11)$$

Where:  $p_0$ : is the surcharge,  $Y_i, Y_j$ : is the unit weight of the soil layers located above the tunnel.

#### 4.1.2 Settlement

According to Chen *et al.* (2012) proper surface settlement estimation is crucial for tunnel construction in highly populated regions since excess surface settlement above the tunnels may cause nearby structures to collapse. Do *et al.* (2014) concluded that the surface settlement caused by the interaction of twin tunnels is anticipated to be higher than that caused by a single tunnel. In this part of results, five points in five sensors positions have been

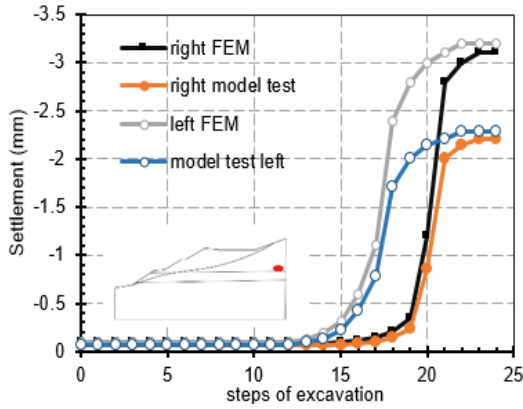


Fig. 14 Settlement in the last tunnel part of the tunnel-sensor point (3)

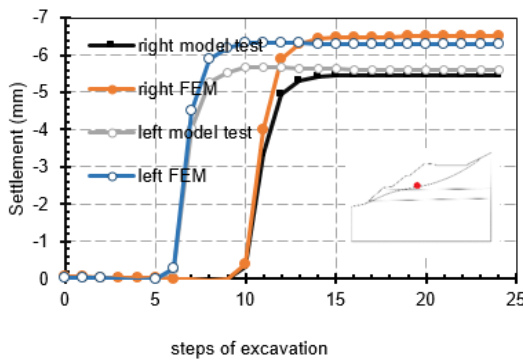


Fig. 15 Settlement in the inclined part of the tunnel sensor point (4)

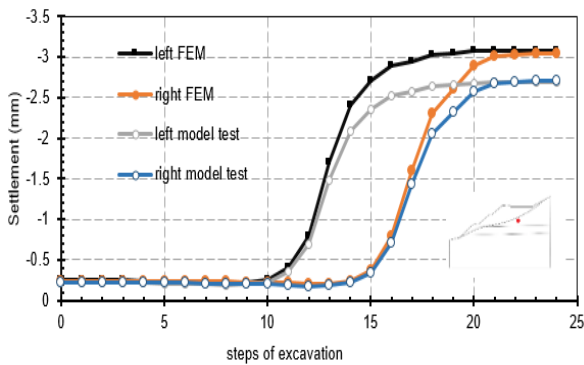
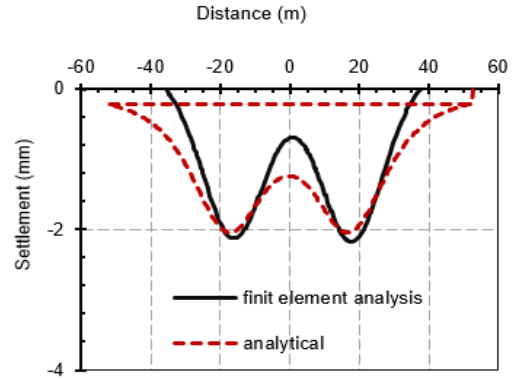
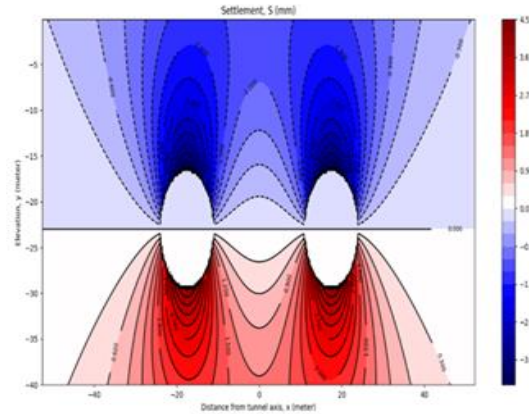


Fig. 16 Settlement under the road-sensor point (5)

appeared. The results show good agreement between the numerical simulation (FEM) and model test. It is obvious that the left tunnel causes more settlement than the right one and this is due to the load transfer mechanism from the right to left tunnel during the excavation, because the first 0.2 m of the left tunnel has been excavated first followed by excavating the left one. Wu *et al.* (2020) concluded that the excavation of the second tunnel led to stress relaxation within the middle pillar, and this indicates to the load transferred from the new tunnel to the existing one. Figs. 12-14 show the settlement directly above the tunnel. While the next two charts in Figs. 15, 16 show settlement little far from the tunnel. It can be shown that the settlement in the sensor position (1) cause the minimum value between the



(a) Verification the analytical solution with numerical simulation



(b) The contour settlement by programming language  
Fig. 17 The results of using analytical solution

other monitoring points. This due to the lower cover depth in the beginning of the slope.

#### 4.1.3 Verification the settlement with analytical solution

The analytical solution has been used to make verification with the numerical one (FEM) analysis. According to the previously mentioned formula, the value of settlement seems to be almost the same as the finite element method. Still there is deviation in the centerline of the tunnel due to slope effect. Fig. 17(a) shows the verification for the surface settlement between the numerical simulation and the analytical solution. While, Fig. 17(b) shows the contour settlement which has been accomplished by using python programming language.

#### 4.2 Plate-slope (numerical simulation- model test)

Rows of plates were utilized as a support to examine the impact of digging two parallel tunnels inside a supported slope. The placement of the rows has been shown in previous mentioned chart. The results will be shown in the following parts:

##### 4.2.1 Vertical stresses

Five points for monitoring the vertical stresses have been shown in this section. The first one Fig. 18 is in the sensor position (1), it is clear that in this point the stress has

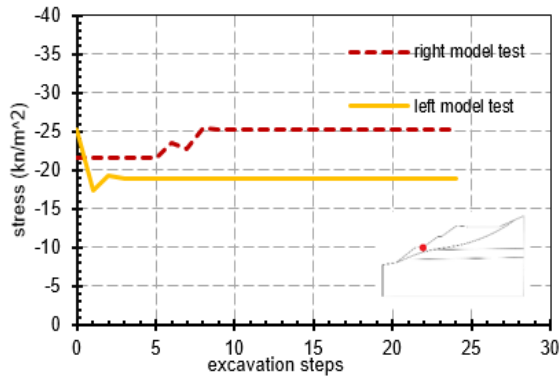


Fig. 18 Stresses in the first part of the tunnel-sensor point (1)

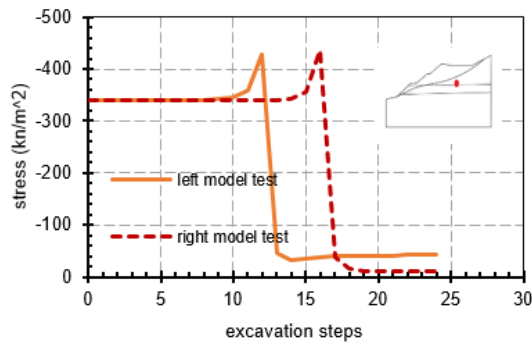


Fig. 19 Stresses in the middle part of the tunnel-sensor point (2)

been increased after dropping down. And this is due to the existence of the plate near this point in the first part of the slope. The presence of the plate makes stress re-distribution and cause the stresses to increase and concentrate in the tunnel lining after decreasing. And this is the difference between the plate supported case and the no support (previous case). Because in the no support case the stress has been increased after the excavation. While, here in this case the stresses have been decreased then increased. In the remaining charts, the stress will increase before the excavation then drop down when the excavation reaches the monitored point. The charts (18-20) represent the sensors points (1-3). While the next two charts in Figs. 21, 22 are little far from the lining.

#### 4.2.2 Settlement

Five monitoring points in five sensors points have been studied in this section. The first in Fig. 23 depicts the settlement in the sensor position (1). While in Fig. 24 the chart depicts the soil movement in the sensor (2) position. Fig. 25 shows the settlement in the sensor position (3). the next chart shows the settlement in the plate support position (4). By comparing between the settlement in sensor (4) position in the plate supported slope Fig. 26 and no support Fig. 14. It can be concluding that the plate can reduce the settlement in its position. While in other places of the slope the settlement will stay the same. The charts (23-25) show the settlement directly above the tunnel. While, the next two charts (26,27) represent the settlement little far from the tunnel lining.

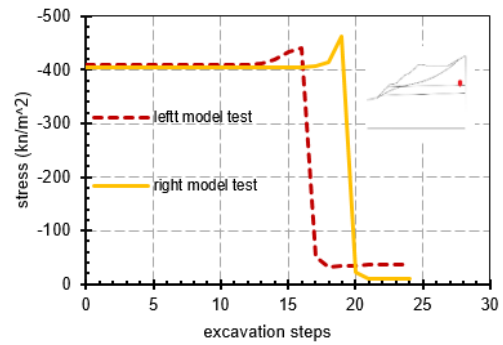


Fig. 20 Stresses in the last tunnel part of the tunnel-sensor point (3)

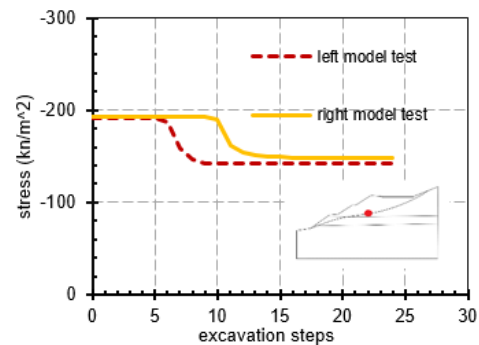


Fig. 21 Stresses in the inclined part of the slope-sensor point (4)

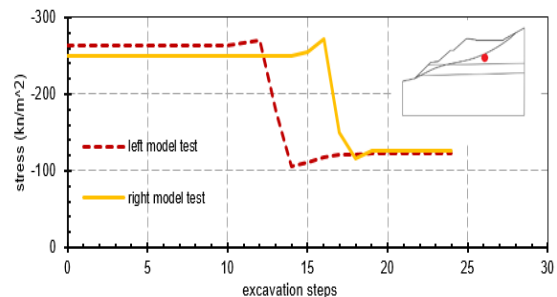


Fig. 22 Stresses under the road-sensor point (5)

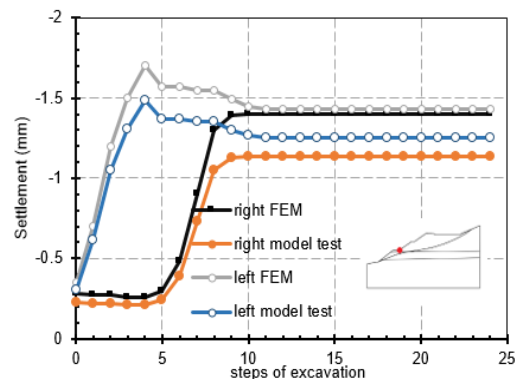


Fig. 23 Settlement in the first tunnel-sensor point (1)

## 5. Discussion

Many parts will be introduced in the discussion, to explain the difference in using different type of support, as

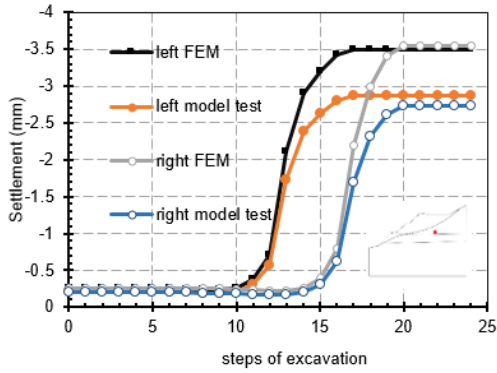


Fig. 24 Settlement in the middle tunnel-sensor point (2)

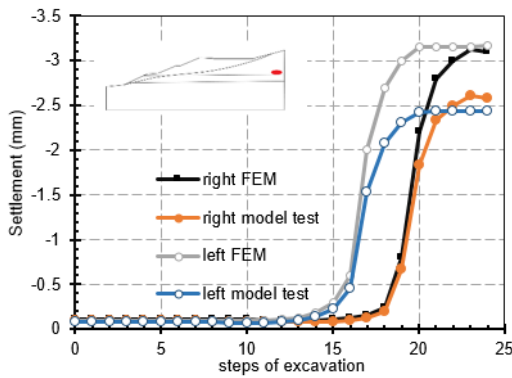


Fig. 25 Settlement in the last tunnel part of the tunnel-sensor point (3)

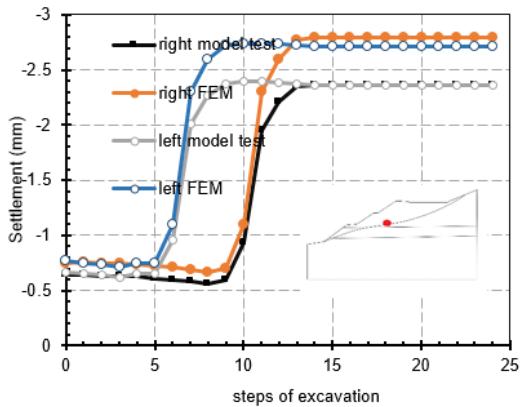


Fig. 26 Settlement in the inclined part of the tunnel-sensor point (5)

the following:

**5.1 Comparison between plate supported slope and no support**

Fig. 28 shows the difference in displacement values in the left and right tunnel in two cases (plate support and no support) in the five monitoring points (five sensors). From the bar chart it is obvious that when using the plate as a support, the displacement will not be less in the whole slope. For example, in the sensor number (4) the displacement in the none supported slope is 5.6 mm and 5.4 mm in the left and right tunnel respectively. While in the

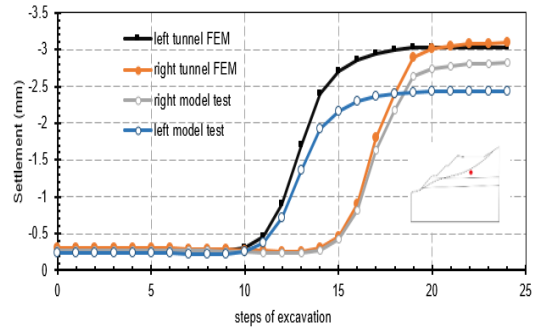
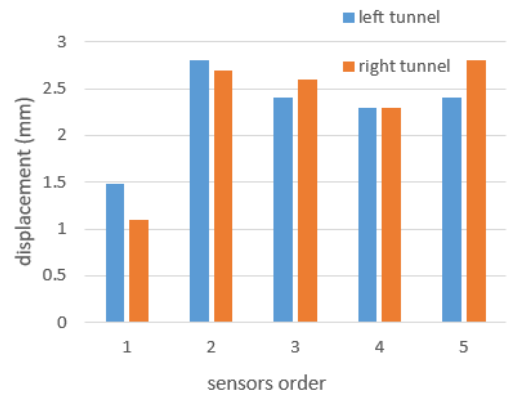
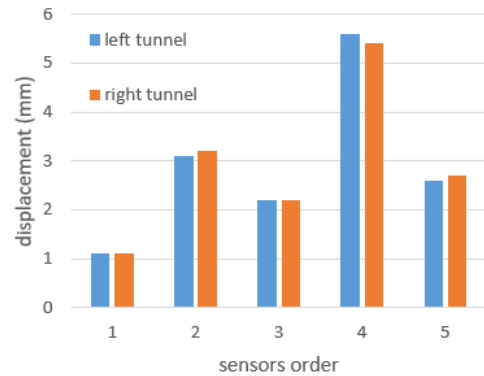


Fig. 27 Settlement under the road-sensor point (5)



(a) Displacement in plate supported slope



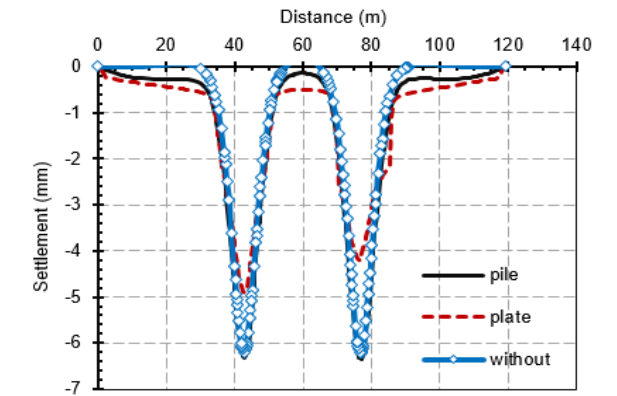
(b) Displacement in no support slope

Fig. 28 Difference in displacement value between support and no support

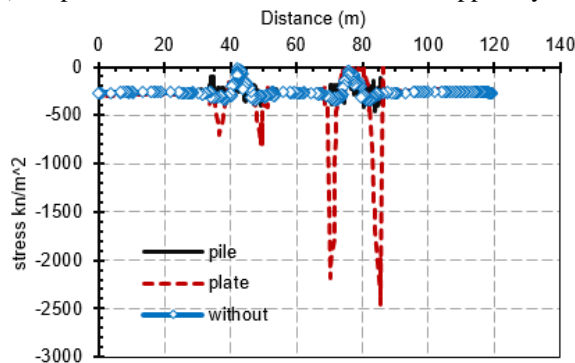
same place in the plate supported slope, the displacement will be 2.3 mm for both tunnels. whereas in another point such as sensor number (1), the displacement in the none supported slope is 1.1 mm in both tunnels. While, it will be 1.48 mm and 1.1 mm for the left and right tunnel respectively. As a conclusion for this part, it can be said that after placing the plates as a supporting system, the factor of safety will increase but the displacement will not decrease in the whole slope. Thus, the support system will influence the safety at the top of the slope, which not leads to get less displacement in the whole slope.

**5.2 Comparison between plate, pile and no support in supported position**

The differences between using various support systems

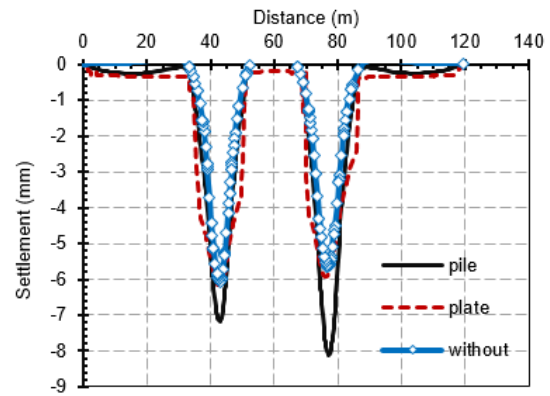


(a) Displacement difference in difference support system

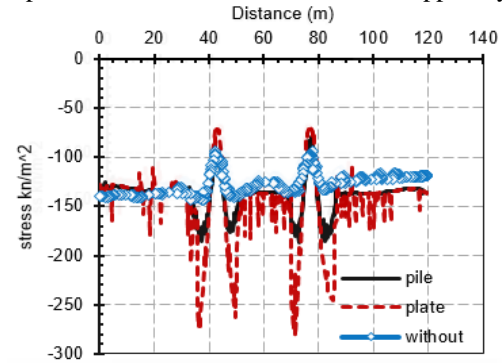


(b) Stress difference in different support system

Fig. 29 Difference between supporting system (plate-pile) and no support system



(a) Displacement difference in difference support system



(b) Stress difference in different support system

Fig. 30 Difference between supporting system (plate-pile) and no support system

in the position of support placement will be illustrated in this section. Fig. 29 show the difference in using piles, plate, and excavate the slope without support. These sections have been taken in the position of the first row of plates and piles in the top of the slope. Fig. 29(a) shows the displacement in this section, it is clear that using the plate cause less settlement than using piles. While the piles and no support give almost the same settlement. In Fig. 29(b) shows the vertical stresses. It is obvious that the plate causes the maximum stress value due to stress concentration between the lining and the plate and this has been noticed through the model test after the installation of the plates. Fig. 30 shows the difference in using the two previous mentioned support system and no support system in the first row position in the middle of the slope. In this position the plate support system and no support cause the same settlement as shown in Fig. 30(a). while in Fig. 30(b) shows the vertical stresses in this section, it shows that the plates and piles cause the same stresses. While the none support system cause less stress. Which leads to consider the slope support system which will be used, will not cause the displacement to be less. In addition, it cannot consider that there is a specific support system will be responsible for reducing the settlement. Instead, each supporting system has its own characteristics depends on the supporting system geometry and stiffness. Fig. 31 shows the difference in contour settlement when using the supporting system and no support system in the position of the first row of the support. It is obvious that using the piles make the

settlement narrower and long above the tunnels, while the plates make the maximum settlement concentrate in specific area above the tunnel as shown in Fig. 31(b). while in the no support system the settlement spread over the tunnels with overlapping. Fig. 32 shows the difference in contour settlement depending on the support systems variation in the first row of the middle plates group. It is very crucial to mention that after extensive parametric study related to the row position of the used support system (plates, piles), which cannot be shown in this paper due to limit space, and after a detailed study to the settlement mechanism and stresses distribution during the excavation process it found that the most suitable place for the support system rows located in the upper part of the slope. Thus, putting the support system in the upper part leads to reduce the settlement and to more economical solution than distributing the support system along the whole slope. In addition, after discovering the distribution of the contour settlement lines it can be conclude even the difference in the piles and plates as a support function, using the plates as a support system is better and cause less settlement than using piles. Figs. 31, 32 show the contour settlement, the main reason for introducing these cross sections in the previous mentioned figures are to show the effect of the support system. Because the previous sections have been taken in the position of the support system.

### 5.3 Comparison between plate pile no support in none supported place

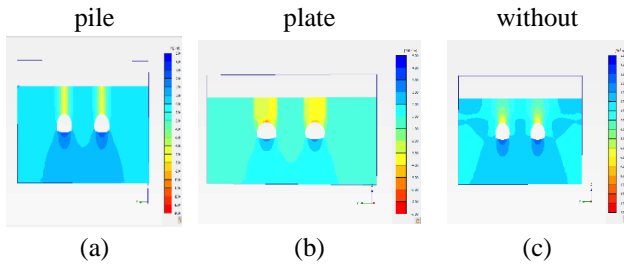


Fig. 31 Difference in contour settlement between the two supported system and no support

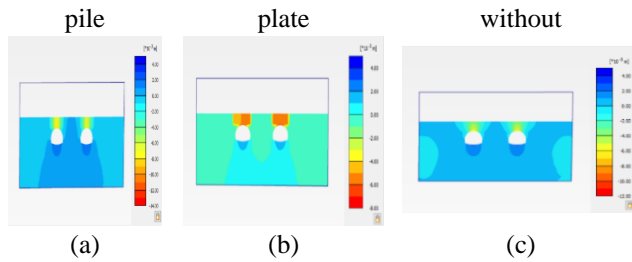
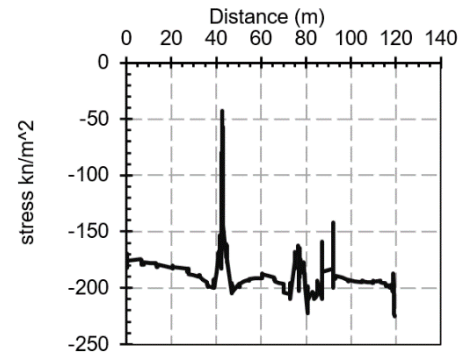


Fig. 32 Difference in contour settlement between the two supported system and no support

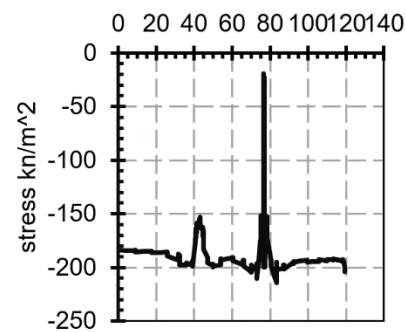
Fig. 33 shows the vertical stresses in none supported section of the slope (whereas no support) in three scenarios: (1): pile support system. (2): plate support system. (3): no support. By comparing the three charts, it can be observed that the stress variation is almost the same in the three cases. However, the stress release in the case of supporting the slope is more than the case where is no support. Which means that the support system such as a piles and plates make stress concentration in the place of placement and this cause stress redistribution to other positions. In other words, the changing of the stress range in the case of no support located between (150-200)  $\text{kn/m}^2$ . While in the case of using plates or piles the range of the vertical stress located between (50-200)  $\text{kn/m}^2$ .

#### 5.4 General discussion

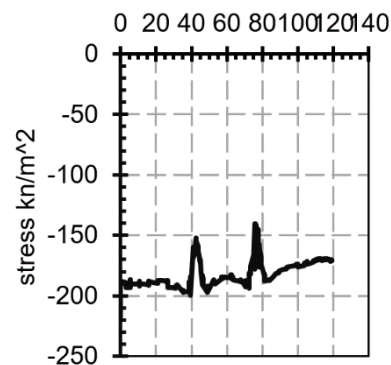
To investigate twin tunnels interaction problem within supported and unsupported slope and in order to create a comparison in this topic, three examples were examined, each with a distinct structure. The following are the scenarios: (1) digging the two parallel tunnels inside an unsupported slope (no plate, no pile) (2) digging the twin tunnels inside the slope that is supported (plate). (3) digging the twin tunnels inside the slope that is supported (piles). The vertical stresses in both the left and right tunnels before the excavation operation is shown in these Fig. 34 (a), (b). The range of the vertical stresses in both tunnels are from (80-600)  $\text{kn/m}^2$ . Which means that this range is increasing along the slope due to increase the cover depth above the tunnels. The vertical stresses value ( $\sigma_z$ ) was almost the same, the plate causing greater stress owing to its weight, followed by the piles, and finally the case without any support causing fewer vertical stresses. And this is logic and relies on the Wight of each structure, the plate weight is more than the piles (soil between each two piles). While, in



(a) Pile support  
Distance (m)



(b) Plate support  
Distance (m)



(c) No support

Fig. 33 the stresses variation in presence of different support system

the none-supported slope there is no structure (no plates-no piles) which leads to less weight and less stresses. Three sections for the three studied cases (three scenarios) have been considered in each part of Fig. 34. These sections are long sections in the center of the left and right tunnel. The charts ((34, c) (34, d)) show the vertical stresses after excavation in three cases: with piles, without support and with plates. The results show that after excavation, the vertical stresses are almost the same due to release stresses. As a result, putting a structure in a slope has a minimal impact on stress release, particularly because the vertical stress after excavation are almost the same. After and before excavation, the vertical stresses were compared, it appears that before excavation, the stresses were arranged according to the Wight of each structure, while after excavation, the action of excavating (the action of movement) cause to re-

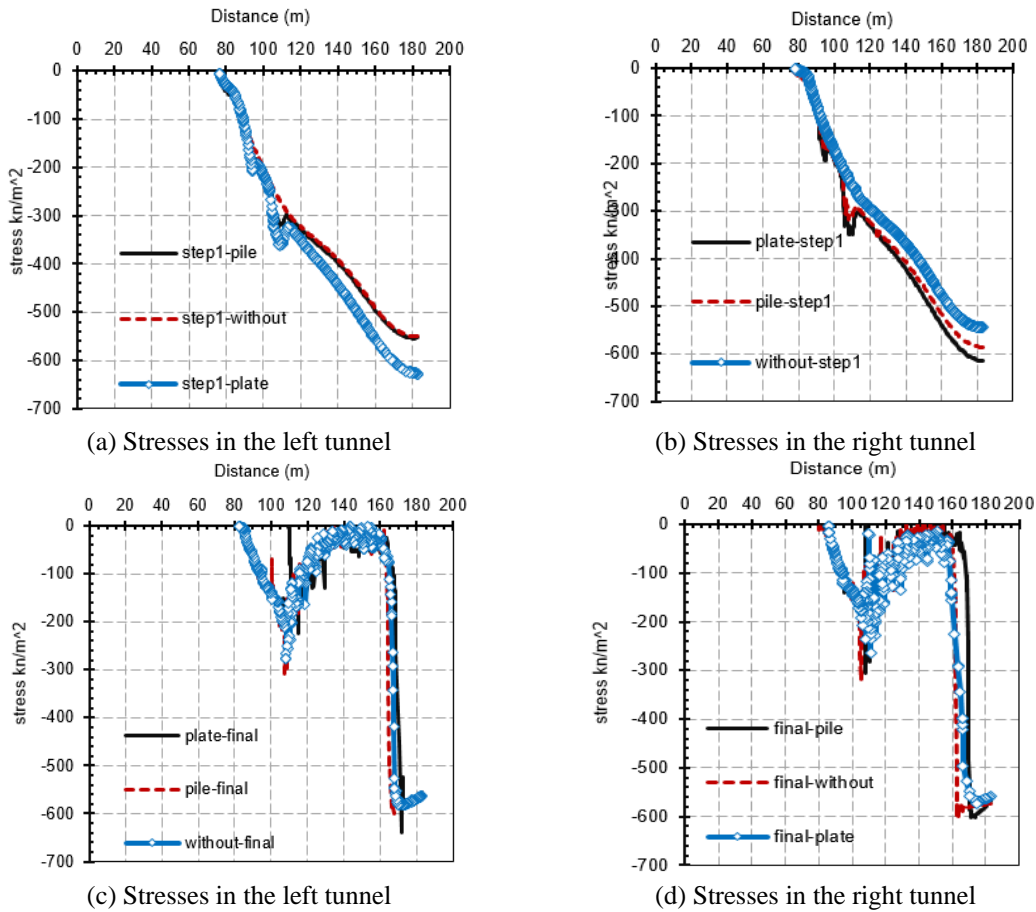


Fig. 34 General stress in the center axis of the left and right tunnel

distribute the stresses which cause to get different arrangement of the stresses, without depending on the structures Wight, and this happened with Zheng *et al.* (2021) who said tunneling process led to convergence of the tunnel periphery towards opening and thus cause the redistribution and release of the surrounding soil stress. In addition, it is obvious that the non-excavated part has the maximum value of stresses due to soil weight (no stress release). In general, during tunneling process the original stress equilibrium of the surrounding soil was destroyed. The soil was deformed under the action of ground stress, resulting in stress redistribution (Yang *et al.* 2019). Thus the redistribution of the stresses along the slope during the excavation action cause different settlement in different part of the slope. This related to the fact that that tunneling necessarily causes stress and deformation, and that the stress changes in the soil caused by tunnel excavation would also produce excessive ground displacement (Ng *et al.* (2013), Lu *et al.* (2019)).

Fig. 35 shows the difference between the horizontal displacement ( $u_x$ ) in the piles and plates. Two figures for each case of the pile has been taken, the first when the pile near the excavation, the second when the pile is far from the excavation. When the support system (piles and plates) on the side part of the slope (not between or above the tunnels) the displacement of the “near pile” will be equal to the displacement of the plate near the excavation. while the plates ‘displacement in the far side of excavation will be

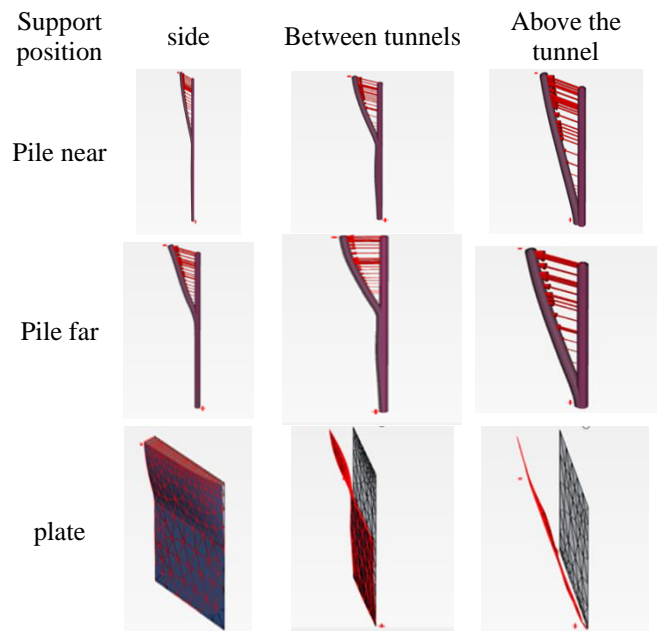


Fig. 35 Difference in the horizontal settlement of the piles and plates in the supported system

equal to the displacement of the pile in the far side. For the support system which located directly above the tunnels, it is obvious that the displacement will be along the support system from bottom till reach above. Whereas, when the

piles and plates are located between and on the side, the displacement concentrates on the top portion of the supported system. As a conclusion the behavior of the pile which located near the excavation will be the same as the plate's side which located near the excavation. Furthermore, the displacement of the pile which located far from the excavation will be equal to the plate's side which located far from the excavation. Furthermore, the displacement ( $ux$ ) of the pile and plate when located between the two holes equal to 2.1 mm. While, when the support system located above the tunnel the horizontal displacement was (2.2, 2.3 2.4 mm) for the outer side, inner side and the plate respectively. As a conclusion for this part it can be said that the horizontal movement of the plate support system will be in harmony with piles. The pile which located far from the excavation will move in an equal value to the plate's side which located far from the excavation. And the same will happen to the support system which located near the excavation.

## 6. Conclusions

In this paper, two model tests supported by finite element analysis (FEM) for excavating twin tunnels within a slope have been done. The two aforementioned model experiments comprise two parallel tunnels (twin tunnels) inside an unsupported slope and a slope supported by plates support system. These model tests have been verified by finite element analysis (FEM). In addition to these two cases, a numerical simulation for piles support system have been done, to compare between the excavation action in presence of different support system for the slope. An analytical solution (equation) has also been used to predict the surface settlement. The results show that:

- It was clear that following excavation steps of the non-supported slope, the stress in both the left and right tunnels had grown due to stress concentration in the lining, especially at the beginning of the slope where the high of the cover depth is modest. While, in the plate supported slope although the cover depth is in small high, but the stress has been increased after dropping down and this is due to the presence of the plate near this monitoring point which cause stress re-distribution. Furthermore, due to stress release in both the supported and non-supported slopes, the vertical stresses in the total rest sensors have decreased.
- In general, the left tunnel causes more settlement than the right tunnel, according to both the model test and numerical simulation results. This occurs as a result of the load transfer mechanism from the right tunnel to the left tunnel, which is exacerbated by the fact that the left tunnel was excavated first, followed by the right tunnel. This has been observed in both supported and unsupported slopes.
- In the top part of the slope, the plate provides less settlement; nevertheless, in the middle section of the slope, the plate support system and the unsupported slope give about the same settlement value. This is because the interaction between the tunnel excavation

movement and the plates or piles is less in the upper part of the slope, whereas as the cover depth of the slope decreases, this interaction will increase, causing more interaction between the tunnel excavation process and the support system. As a result, it is suggested that the support system be built in the top portion of the slope without using these support systems in other sections of the slope.

- The slope supported by piles gives the maximum value of settlement in many sections of the slope, thus, the piles' function concentrate in preventing the overlapping between the settlement due to tunnel interaction, and decrease the settlement area. In addition, the plate and pile structures within the slope during excavate the twin tunnels, redistribute the stresses, thus it is not necessary to get the less settlement due to use piles or plate as a slope support technique in each section of the slope.
- The piles and plates causes more stresses in its position and cause stress concentration in the area between the lining and the support system, thus a variation in the vertical stresses values will be created in comparison with the unsupported position of the slope, which leads to different distribution of the stresses along the slope while excavating twin tunnels. However, the effect of using plate or piles is limited in the position of the piles or plate thus the other places of the slope will not be affected by these structures.
- As a conclusion, the best usage of the support system is placing the rows of plates in the upper part of the slope. Especially because the plates reduce the settlement more than the piles.
- The main factors which affect the stress and settlement distribution, are the cover depth of the slope because less cover depth leads to more interaction between the support system and the excavation process, the movement during excavation, the structures which are buried in the slope such as the lining of the tunnel, the plates or piles and the interaction between all of these components.
- The displacement ( $ux$ ) of the pile near the excavation equal to the displacement of the plate's side near the excavation, and the same happened to the far side of the excavation. Furthermore, the displacement of the pile which located above the tunnel near the inner side was almost (2.3) mm and (2.2) mm when the pile in the outer side. while the displacement of the plate which located above the tunnel was (2.4) mm. In addition, when the plate located between the two tunnels the displacement was (2.1) mm, while when the pile located between the tunnels the displacement was almost the same as the plate from the two side of the tunnels.

## Acknowledgments

This work was supported by the National Key R&D Program of China (Grant No. 581 2018YFC1504802), National Natural Science Foundation of China (Grant No.41972266).

## References

- Addenbrooke (1996), "Numerical modelling in stiff clay", Thesis, Imperial College.
- Bobet, A. (2001), "Analytical solutions for shallow tunnels in saturated ground", *J. Eng. Mech.*, **127**(12), 1258-1266. [https://doi.org/10.1061/\(ASCE\)0733-9399\(2001\)127:12\(1258\)](https://doi.org/10.1061/(ASCE)0733-9399(2001)127:12(1258)).
- Chakeri, H., Hasanpour, R., Hindistan, M.A. and Ünver, B. (2011), "Analysis of interaction between tunnels in soft ground by 3D numerical modeling", *Bull. Eng. Geol. Environ.*, **70**, 439-448. <https://doi.org/10.1007/s10064-010-0333-8>.
- Channabasavaraj, W. and Visvanath, B. (2013), "Influence of relative position of the tunnels: A numerical study on twin tunnels", *CARE Conference*, Chicago, America.
- Chen, R.P., Zhu, J., Liu, W. and Tang, X.W. (2011), "Ground movement induced by parallel EPB tunnels in silty soils", *Tunnel. Undergr. Space Technol.*, **26**(1), 163-171. <https://doi.org/10.1016/j.tust.2010.09.004>.
- Chen, S.L., Gui, M.W. and Yang, M.C. (2012), "Applicability of the principle of superposition in estimating ground surface settlement of twin-and quadruple-tube tunnels", *Tunnel. Undergr. Space Technol.*, **28**, 135-149. <https://doi.org/10.1016/j.tust.2011.10.005>.
- Chen, S.L., Lee, S.C. and Gui, M.W. (2009), "Effects of rock pillar width on the excavation behavior of parallel tunnels", *Tunnel. Undergr. Space Technol.*, **24**(2), 148-154. <https://doi.org/10.1016/j.tust.2008.05.006>.
- Choi, J.I. and Lee, S.W. (2010), "Influence of existing tunnel on mechanical behavior of new tunnel", *Geomech. Eng.*, **14**(5), 773-783. <https://doi.org/10.12989/gae.2020.22.6.497>.
- Cording, E.J. and Hansmire, W.H. (1975), "Displacement around soft ground tunnels", *Proceedings of the Pan-American Conference of Soil Mechanics and Foundation Engineering*, Vol. 4, Mexico.
- Do, N.A., Dias, D. and Oreste, P. (2014), "Three-dimensional numerical simulation of a mechanized twin tunnels in soft ground", *Tunnel. Undergr. Space Technol.*, **42**, 40-51. <https://doi.org/10.1016/j.tust.2014.02.001>.
- Elwood, D.E. and Martin, C.D. (2016), "Ground response of closely spaced twin tunnels constructed in heavily overconsolidated soils", *Tunnel. Undergr. Space Technol.*, **51**, 226-237. <https://doi.org/10.1016/j.tust.2015.10.037>.
- Franzius, J.N., Potts, D.M. and Burland, J.B. (2005), "The influence of soil anisotropy and K<sub>0</sub> on ground surface movements resulting from tunnel excavation", *Géotechnique*, **55**(3), 189-199. <https://doi.org/10.1680/geot.2005.55.3.189>
- Fumagalli, E. (2013), *Statical and Geomechanical Models*, Springer Science & Business Media.
- Gao, S.M., Chen, J.P., Zuo, C.Q. and Wang, W. (2017), "Monitoring of three-dimensional additional stress and strain in shield segments of former tunnels in the construction of closely-spaced twin tunnels", *Géotechnique*, **35**(1), 69-81. <https://doi.org/10.1007/s10706-016-0085-8>.
- Hong, Y., Soomro, M.A. and Ng, C.W.W. (2015), "Settlement and load transfer mechanism of pile group due to side-by-side twin tunnelling", *Comput. Geotech.*, **64**, 1051-19. <https://doi.org/10.1016/j.compgeo.2014.10.007>.
- Huang, F., Zhu, H., Xu, Q. and Cai, Y. (2013), "The effect of weak interlayer on the failure pattern of rock mass around tunnel—Scaled model tests and numerical analysis", *Tunnel. Undergr. Space Technol.*, **35**, 207-218. <https://doi.org/10.1016/j.tust.2012.06.014>.
- Jiang, Y. (1993), "Theoretical and experimental study on the stability of deep underground opening", PhD Thesis.
- Kim, J.W. (2012), "A study on the stability of asymmetrical twin tunnels in alternating rock layers using scaled model tests", *Tunnel. Undergr. Space Technol.*, **22**(1), 22-31. <https://doi.org/10.7474/TUS.2012.22.1.022>.
- Li, B. and Ji, F. (2017), "Analysis of the influence of shield construction on the surrounding ground surface settlement", *2016 International Conference on Engineering Management (Iconf-EM 2016)*, January.
- Li, X., Du, S. and Zhang, D. (2013), "Numerical simulation of the interaction between two parallel shield tunnels", *ICPTT 2012: Better Pipeline Infrastructure for a Better Life*, Wuhan, China.
- Loganathan, N. and Poulos, H.G. (1998), "Analytical prediction for tunneling-induced ground movements in clays", *J. Geotech. Geoenviron. Eng.*, **124**(9), 846-856. [https://doi.org/10.1061/\(ASCE\)1090-0241\(1998\)124:9\(846\)](https://doi.org/10.1061/(ASCE)1090-0241(1998)124:9(846)).
- Lu, H., Shi, J., Wang, Y. and Wang, R. (2019), "Centrifuge modeling of tunneling-induced ground surface settlement in sand", *Undergr. Space*, **4**(4), 302-309. <https://doi.org/10.1016/j.undsp.2019.03.007>.
- Lü, X., Zhou, Y., Huang, M. and Zeng, S. (2018), "Experimental study of the face stability of shield tunnel in sands under seepage condition", *Tunnel. Undergr. Space Technol.*, **74**, 195-205. <https://doi.org/10.1016/j.tust.2018.01.015>.
- Meguid, M.A., Saada, O., Nunes, M.A. and Mattar, J. (2008), "Physical modeling of tunnels in soft ground: A review", *Tunnel. Undergr. Space Technol.*, **23**(2), 185-198. <https://doi.org/10.1016/j.tust.2007.02.003>.
- Mortazavi, A., Hassani, F.P. and Shabani, M. (2009), "A numerical investigation of rock pillar failure mechanism in underground openings", *Comput. Geotech.*, **36**(5), 691-697. <https://doi.org/10.1016/j.compgeo.2008.11.004>.
- Nematollahi, M. and Dias, D. (2019), "Three-dimensional numerical simulation of pile-twin tunnels interaction—Case of the Shiraz subway line", *Tunnel. Undergr. Space Technol.*, **86**, 75-88. <https://doi.org/10.1016/j.tust.2018.12.002>.
- Nematollahi, M. and Dias, D. (2020), "Interaction between an underground parking and twin tunnels—Case of the Shiraz subway line", *Tunnel. Undergr. Space Technol.*, **95**, 103150. <https://doi.org/10.1016/j.tust.2019.103150>.
- Ng, C.W., Boonyarak, T. and Mašin, D. (2013), "Three-dimensional centrifuge and numerical modeling of the interaction between perpendicularly crossing tunnels", *Can. Geotech. J.*, **50**(9), 935-946. <https://doi.org/10.1139/cgj-2012-0445>.
- Ng, C.W., Lee, K.M. and Tang, D.K. (2004), "Three-dimensional numerical investigations of new Austrian tunnelling method (NATM) twin tunnel interactions", *Can. Geotech. J.*, **41**(3), 523-539. <https://doi.org/10.1139/t04-008>.
- Ng, C.W.W., Lu, H. and Peng, S.Y. (2013), "Three-dimensional centrifuge modelling of the effects of twin tunnelling on an existing pile", *Tunnel. Undergr. Space Technol.*, **35**, 189-199. <https://doi.org/10.1016/j.tust.2012.07.008>.
- Ocak, I. (2013), "Interaction of longitudinal surface settlements for twin tunnels in shallow and soft soils: The case of Istanbul Metro", *Environ. Earth Sci.*, **69**(5), 1673-1683. <https://doi.org/10.1007/s12665-012-2002-7>.
- Oliaei, M. and Manafi, E. (2015), "Static analysis of interaction between twin-tunnels using discrete element method (DEM)", *Scientia Iranica*, **22**(6), 1964-1971.
- Peck, R.B. (1969), "Deep excavation and tunneling in soft ground", *Proceedings of the 7th ICSMFE*, 225-290..
- Rowe, R.K., Lo, K.Y. and Kack, G.J. (1983), "A method of estimating surface settlement above tunnels constructed in soft ground", *Can. Geotech. J.*, **20**(1), 11-22. <https://doi.org/10.1139/t83-002>.
- Seo, H.J., Choi, H., Bae, G. and Lee, I. (2014), "Pillar-reinforcement technology beneath existing structures: Small-scale model tests", *KSCSE J. Civil Eng.*, **18**(3), 819-826. <https://doi.org/10.1007/s12205-014-1392-3>.
- Shi, J., Zhang, X., Chen, Y. and Chen, L. (2020), "Numerical

- parametric study of countermeasures to alleviate the tunnel excavation effects on an existing tunnel in a shallow-buried environment near a slope”, *Appl. Sci.*, **10**(2), 608. <https://doi.org/10.3390/app10020608>.
- Shivaei, S., Hataf, N. and Pirastehfar, K. (2020), “3D numerical investigation of the coupled interaction behavior between mechanized twin tunnels and groundwater—A case study: Shiraz metro line 2”, *Tunnel. Undergr. Space Technol.*, **103**, 103458. <https://doi.org/10.1016/j.tust.2020.103458>.
- Soomro, M.A. (2021), “3D finite element analysis of effects of twin stacked tunnels at different depths and with different construction sequence on a piled raft”, *Tunnel. Undergr. Space Technol.*, **109**, 103759. <https://doi.org/10.1016/j.tust.2020.103759>.
- Soomro, M.A., Kumar, M., Xiong, H., Mangnejo, D.A. and Mangi, N. (2020), “Investigation of effects of different construction sequences on settlement and load transfer mechanism of single pile due to twin stacked tunnelling”, *Tunnel. Undergr. Space Technol.*, **96**, 103171. <https://doi.org/10.1016/j.tust.2019.103171>.
- Soomro, M.A., Ng, C.W.W., Liu, K. and Memon, N.A. (2017), “Pile responses to side-by-side twin tunnelling in stiff clay: Effects of different tunnel depths relative to pile”, *Comput. Geotech.*, **84**, 101-116. <https://doi.org/10.1016/j.compgeo.2016.11.011>.
- Sun, X., Chen, F., Miao, C., Song, P., Li, G., Zhao, C. and Xia, X. (2018), “Physical modeling of deformation failure mechanism of surrounding rocks for the deep-buried tunnel in soft rock strata during the excavation”, *Tunnel. Undergr. Space Technol.*, **74**, 247-261. <https://doi.org/10.1016/j.tust.2018.01.022>.
- Suwansawat, S. and Einstein, H. (2007), “Describing settlement troughs over twin tunnels using a superposition technique”, *J. Geotech. Geoenviron. Eng.*, **133**(4), 445-468. [https://doi.org/10.1061/\(ASCE\)1090-0241\(2007\)133:4\(445\)](https://doi.org/10.1061/(ASCE)1090-0241(2007)133:4(445)).
- Taylor, R.N. (1984), “Ground movements associated with tunnels and trenches”, Ph. D. Thesis, University of Cambridge.
- Vlachopoulos, N. and Vazaios, I. (2015), “Case study: The influence of tunnelling on slope stability”, *Conference of GeoQuebec 2015*, Quebec, Canada.
- Wang, Z., Yao, W., Cai, Y., Xu, B., Fu, Y. and Wei, G. (2019), “Analysis of ground surface settlement induced by the construction of a large-diameter shallow-buried twin-tunnel in soft ground”, *Tunnel. Undergr. Space Technol.*, **83**, 520-532. <https://doi.org/10.1016/j.tust.2018.09.021>.
- Wu, L., Zhang, X., Zhang, Z. and Sun, W. (2020), “3D discrete element method modelling of tunnel construction impact on an adjacent tunnel”, *KSCE J. Civil Eng.*, **24**(2), 657-669. <https://doi.org/10.1007/s12205-020-2054-2>.
- Yang, J., Liu, C., Chen, Q. and Xie, X. (2017), “Performance of overlapped shield tunneling through an integrated physical model tests, numerical simulations and real-time field monitoring”, *Undergr. Space*, **2**(1), 45-59. <https://doi.org/10.1016/j.undsp.2017.04.002>.
- Yang, W., Wang, M., Zhou, Z., Li, L., Yuan, Y. and Gao, C. (2019), “A true triaxial geomechanical model test apparatus for studying the precursory information of water inrush from impermeable rock mass failure”, *Tunnel. Undergr. Space Technol.*, **93**, 103078. <https://doi.org/10.1016/j.tust.2019.103078>.
- Yun, B. (2019), *Underground Engineering Planning, Design, Construction and Operation of the Underground Space*, Academic Press.
- Zhang, Q., Wang, J., Wang, W., Bai, S. and Lin, P. (2019), “Study on slope stability due to the influence of excavation of the high-speed rail tunnel”, *Nat. Hazard. Risk*, 1193-1208. <https://doi.org/10.1080/19475705.2019.1568311>.
- Zheng, H., Li, P. and Ma, G. (2021), “Stability analysis of the middle soil pillar for asymmetric parallel tunnels by using model testing and numerical simulations”, *Tunnel. Undergr. Space Technol.*, **108**, 103686. <https://doi.org/10.1016/j.tust.2020.103686>.
- Zhu, W.S., Zhang, Q.B., Zhu, H.H., Li, Y., Yin, J.H., Li, S.C., ... & Zhang, L.J.C.G.J. (2010), “Large-scale geomechanical model testing of an underground cavern group in a true three-dimensional (3-D) stress state”, *Can. Geotech. J.*, **47**(9), 935-946. <https://doi.org/10.1139/T10-006>.

IC